Electronic Supplementary Material (ESI) for Nanoscale Advances.

Electronic Supplementary Information (ESI)

Development of Near-Infrared Sensitized Core-Shell-Shell Upconverting Nanoparticles as pH-responsive Probes

Manoj K. Mahata and Kang Taek Lee*

Department of Chemistry, School of Physics and Chemistry, Gwangju Institute of Science and Technology (GIST), Gwangju-61005, South Korea

*Corresponding author: ktlee@gist.ac.kr

Luminescence mechanism upon 980 nm laser light excitation:

The spectra show strong emission bands that appear at 449 nm ($^1D_2 \rightarrow {}^3H_6$), 474 nm ($^1G_4 \rightarrow {}^3H_6$), 643 nm ($^1G_4 \rightarrow {}^3F_4$), and 802 nm ($^3H_4 \rightarrow {}^3H_6$). The weak band at 300 nm is attributed to the $^1I_6 \rightarrow {}^3H_6$ transition. A comparatively strong band in the UV region that appears at 360 nm has a weak shoulder at 343 nm and the emissions are obtained due to the transitions $^1D_2 \rightarrow {}^3H_6$ and $^1I_6 \rightarrow {}^3F_4$. The representative energy level diagram with possible transition pathways are shown in Figure S3a. The energy levels- $^3H_5$, $^3F_3$ ($^3F_2$), $^1G_4$, $^1D_2$ and $^1I_6$ of Tm^{3+} ions are populated by successive energy transfer by the Yb^{3+} ions upon absorbing 980 nm excitation photons. Due to the difference in the energy levels, the dipole-dipole interaction is non-resonance in nature and the processes involve phonon-assisted non-radiative energy transfer through the following ways:

The ground state ions at the $^3H_6$ level are excited to the $^3H_5$ by receiving energy from the adjacent Yb^{3+} ions, which are excited to $^2F_{5/2}$ from $^2F_{7/2}$ under 980 nm laser excitation and excess energy is dissipated by the phonons of the $NaYF_4$ host. Because of shorter lifetime of $^3H_5$ level, the ions relax to $^3F_4$ by multi-phonon absorption. In the next step, the Tm^{3+} ions are excited to the $^3F_2$ level by energy transfer from Yb^{3+} ions' excited state to the $^3F_4$ level. The Tm^{3+} ions may decay nonradiatively to $^3H_4$ level owing to the small difference in energy, following $^3H_4 \rightarrow {}^3H_6$ transition gives NIR emission at 802 nm. Upon energy transfer by the Yb^{3+} ions, the Tm^{3+} ions are excited to $^1G_4$ from $^3F_4$ level and the radiative transitions from this level: $^1G_4 \rightarrow {}^3F_4$ and $^1G_4 \rightarrow {}^3H_6$ produce the red (643 nm) and blue (474 nm) emissions. Successively, the excited Yb^{3+} ions transfer their energy to the $^1D_2$ level of Tm^{3+}. As an alternative way, the population of Tm^{3+} ions at the $^1D_2$ level may include a cross-relaxation (CR) process involving the $^1D_2$, $^3F_3$ and $^3H_6$ levels through- $^3F_3\ (Tm^{3+}) + {}^3F_3\ (Tm^{3+}) \rightarrow {}^3H_6\ (Tm^{3+}) + {}^1D_2\ (Tm^{3+})$. After this process, the blue and UV upconversion emissions occur at 449 nm and 360 nm, respectively due to the $^1D_2 \rightarrow {}^3H_6$ and $^1D_2 \rightarrow {}^3F_4$ transitions. The Tm^{3+} ions are subsequently excited to the $^3P_{1,2}$ levels from $^1D_2$ by another energy transfer from Yb^{3+} to Tm^{3+} ion. However, a rapid population from $^3P_{1,2}$ levels to $^1I_6$ takes place by multiphonon relaxation and the transition corresponding to $^1I_6 \rightarrow {}^3H_6$ results UV upconversion emission at 300 nm. The highly intense NIR emission (802 nm) may include population through cross-relaxation process: $^1G_4$

(Tm^{3+}) + $^3H_6$ (Tm^{3+}) → $^3F_4$ (Tm^{3+}) + $^3F_{2,3}$ (Tm^{3+}), which eventually increases the population of $^3H_4$ level.

Calculation of LRET efficiency:

According to the theory in "Handbook of Biological Confocal Microscopy", J. B. Pawley [1], the fluorescence lifetime of the donor of the LRET pair without acceptor (τ_D), is

$$\tau_D = \frac{1}{k_r + k_{nr}}$$

and the lifetime of the donor in the presence of the LRET counterpart (with acceptor)

$$\tau_{DA} = \frac{1}{k_r + k_{nr} + k_t}$$

where k_r is the rate of the radiative decay of the Tm^{3+} (donor), k_{nr} is the rate of the non-radiative decay of the Tm^{3+} (donor), and k_t is the rate of the energy transfer from Tm^{3+} (donor) to FITC (acceptor).

The LRET efficiency of 16.2% is calculated from the formula

$$E_{LRET} = 1 - \frac{\tau_{DA}}{\tau_D}$$

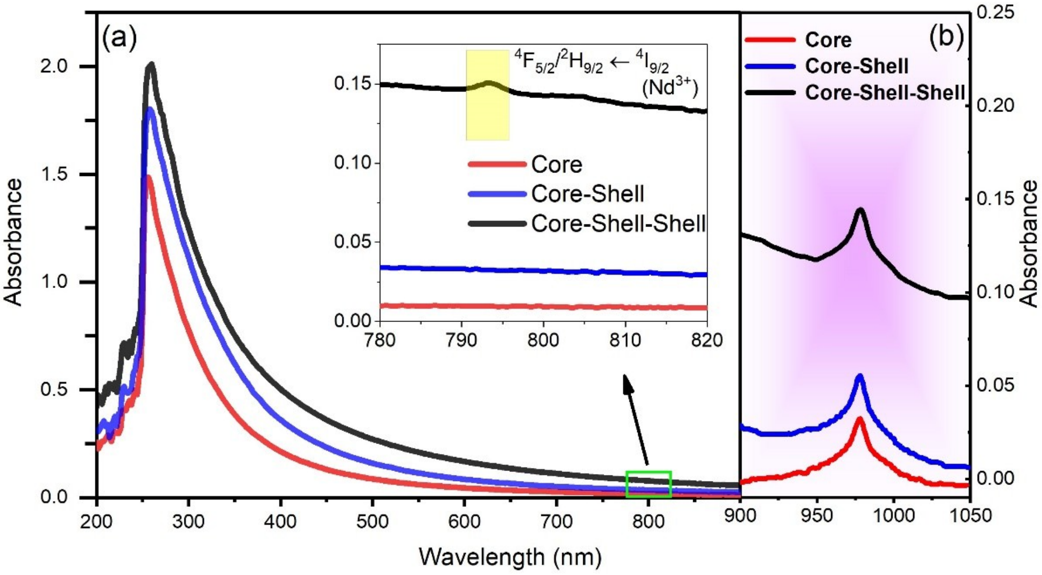

Figure S1. (a) Absorption spectra in hexane of core, core-shell and core-shell-shell nanoparticles 200-900 nm region. Inset shows the enlarged portion around 800 nm wavelength. (b) The absorption spectra at the 900-1050 nm region.

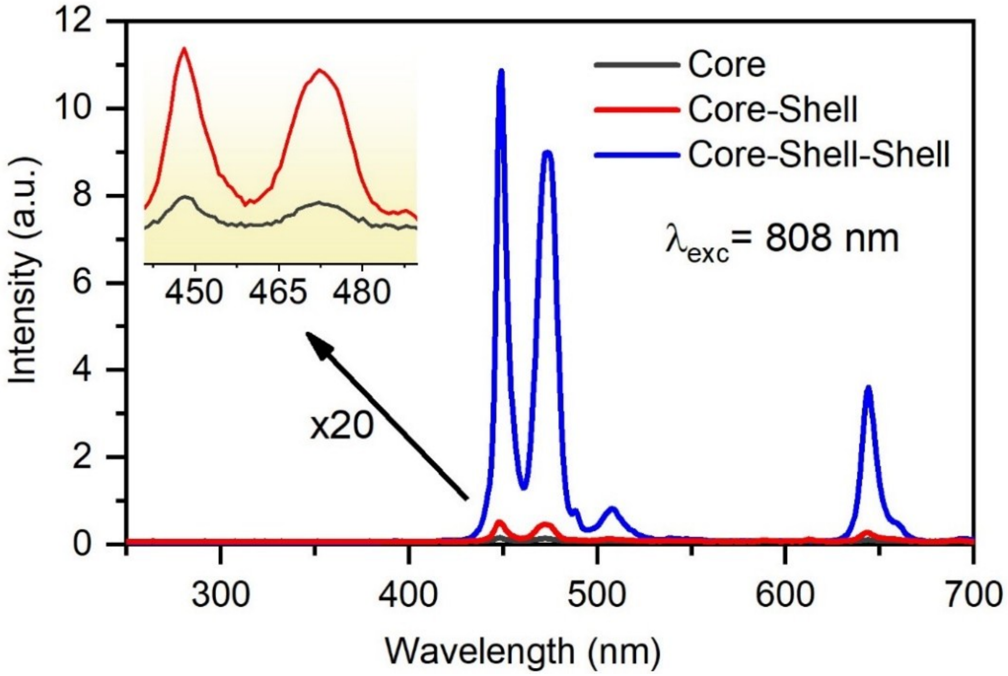

Figure S2. Upconversion luminescence spectra of core ($NaYF_4$:20%Yb^{3+}/0.5%Tm^{3+}), core-shell ($NaYF_4$:20%Yb^{3+}/0.5%Tm^{3+}@$NaYF_4$:15%Yb^{3+}) and core-shell-shell ($NaYF_4$:20%Yb^{3+}/0.5%Tm^{3+}@$NaYF_4$:15%Yb^{3+}@$NaYF_4$:10%Yb^{3+}/20%Nd^{3+}) nanoparticles. The luminescence is enhanced in the core-shell-shell structure due to the sensitization effect by Nd^{3+} ions upon 808 nm excitation light. The inset shows 20 times enlarged peaks of core and core-shell particles. The luminescence measurements were performed in hexane with 500 µg/ml UCNPs concentration.

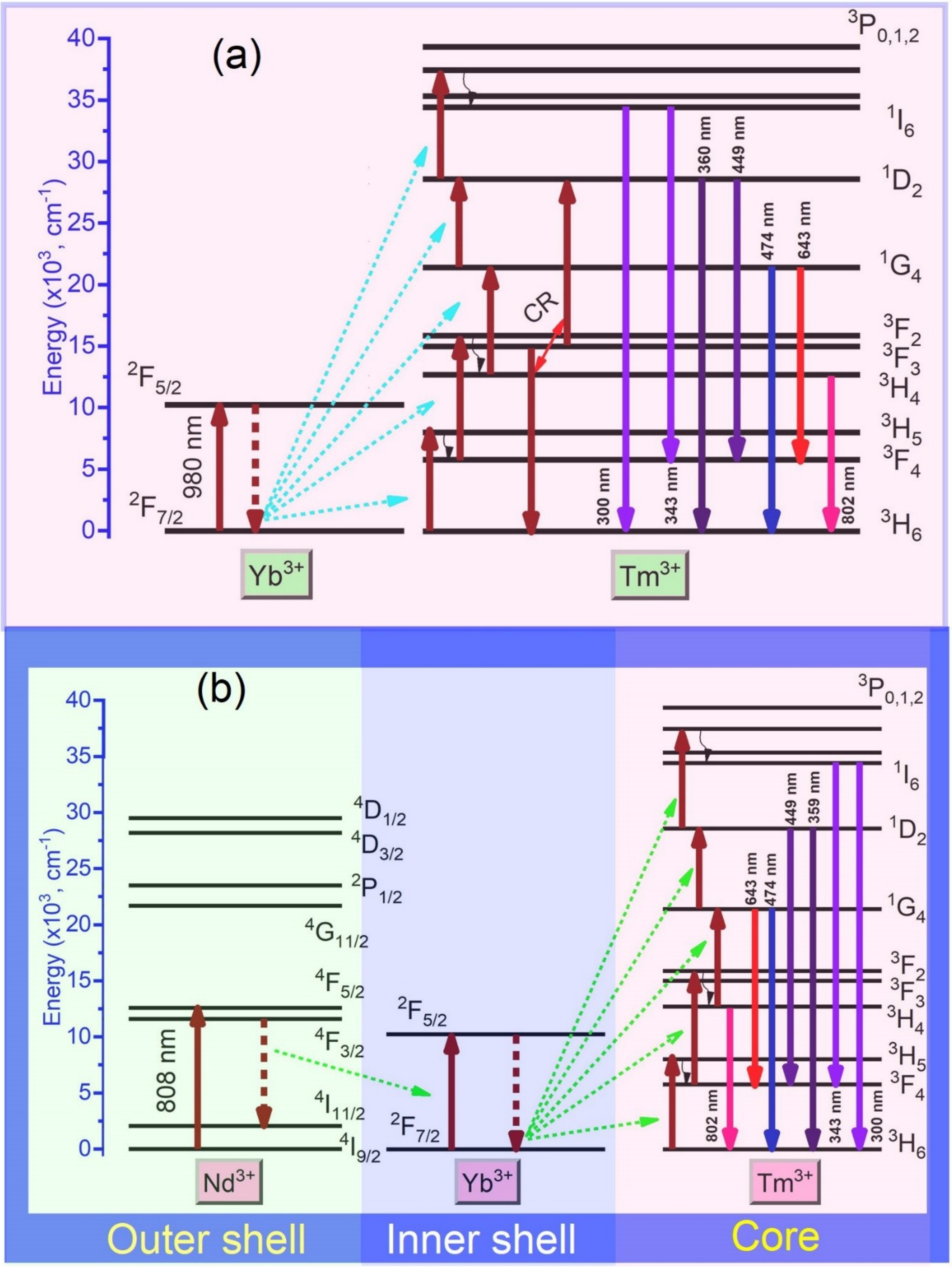

Figure S3. Energy level diagrams and possible transition pathways for (a) Yb^{3+}-Tm^{3+} ions upon 980 nm laser excitation, (b) Nd^{3+}-Yb^{3+}-Tm^{3+} ions upon 808 nm excitation.

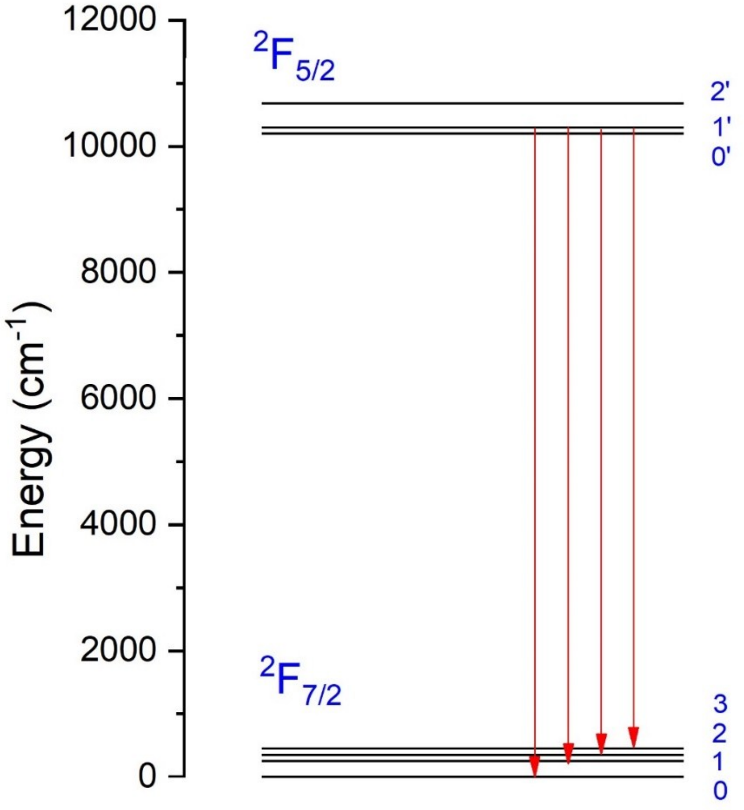

Figure S4. Stark sub-levels of Yb^{3+} ions and possible transitions [2, 3]

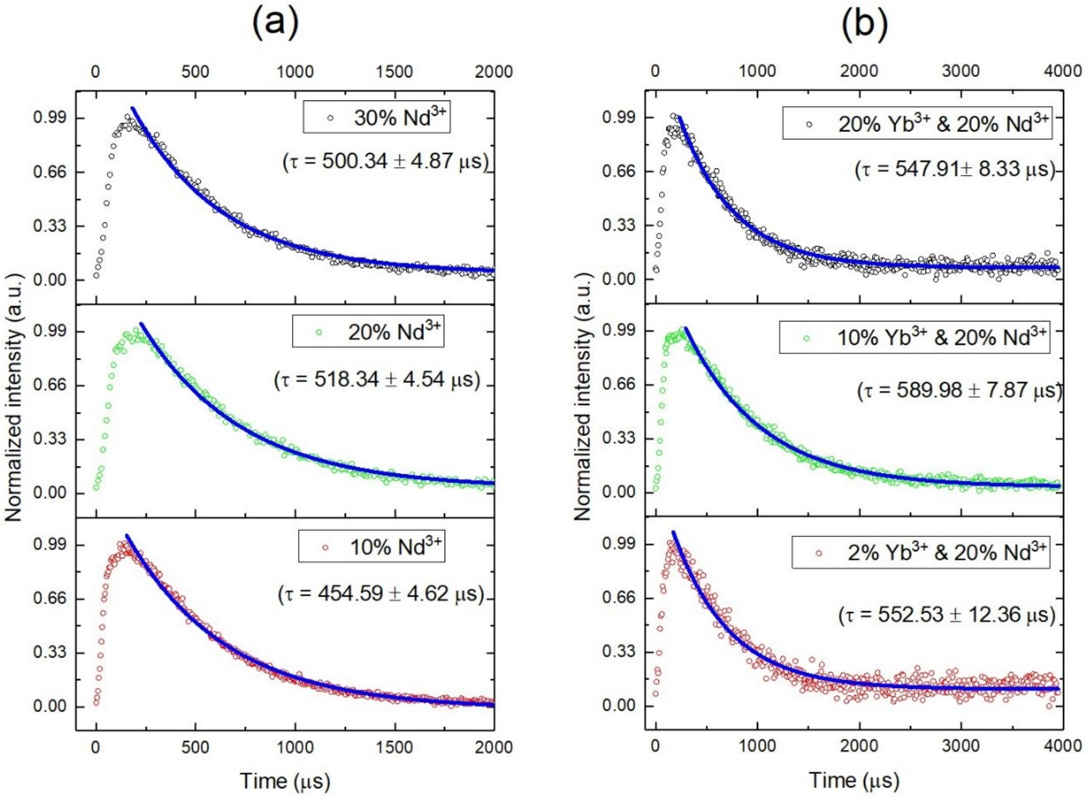

Figure S5. Transients of $^1G_4 \rightarrow ^3H_6$ (474 nm) of Tm^{3+} with variation of (a) Nd^{3+} concentrations (10%, 20% and 30% at the outer shell) and (b) Yb^{3+} concentrations (2%, 10% and 20% at the inner shell) upon 808 nm laser light excitation; all the samples contain 10 mol% of Yb^{3+} ions along with Nd^{3+} ions in the outer shell. The core is $NaYF_4:Yb^{3+}/Tm^{3+}$. The decay curves were fitted by single exponential decay of the type: $y=A_1*\exp(-x/t)+y_0$. The decay times are shown in the respective figures.

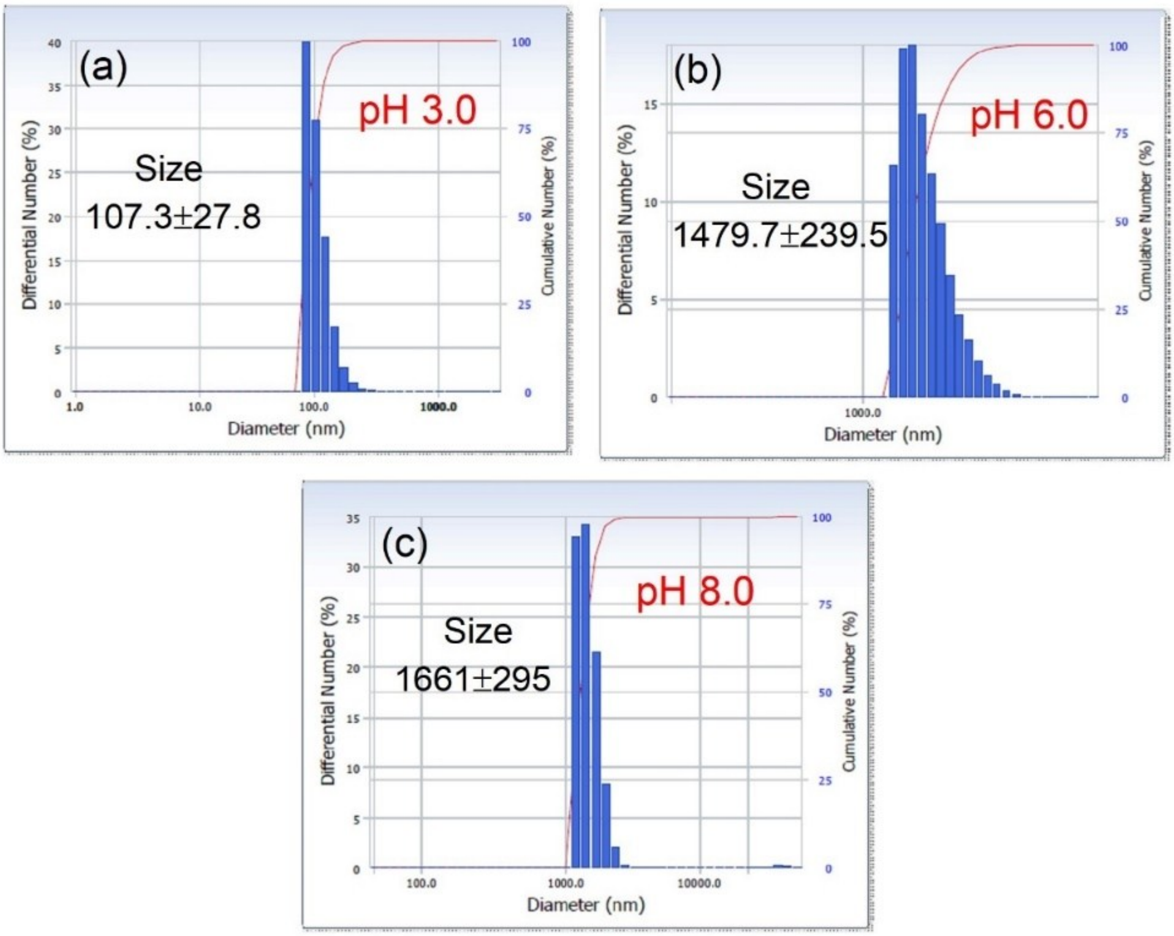

Figure S6. Number weighted Dynamic Light Scattering (DLS) measurements of PEI-modified nanoparticles in different pH buffers. The average size of the nanoparticles is shown in each graph.

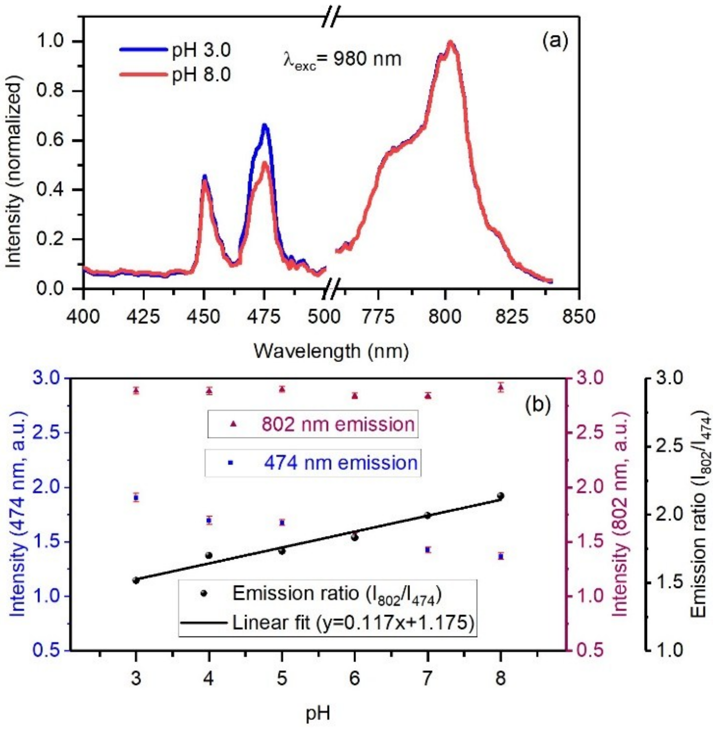

Figure S7. (a) The 802 nm-normalized upconversion spectra of FITC conjugated core-shell-shell nanoparticles upon 980 nm laser excitation (power: 140 mW) at two extreme pH values (3 and 8) (b) evolution of upconversion emission intensity corresponding to 474 nm, 802 nm bands and their intensity ratio (802 to 474 nm) of FITC conjugated core-shell-shell nanoparticles; calculated standard deviations (S.D.) were taken from three measurements; the fitted linear line (black) shows the ratiometric calibration of the two bands (802 to 474 nm) with pH.

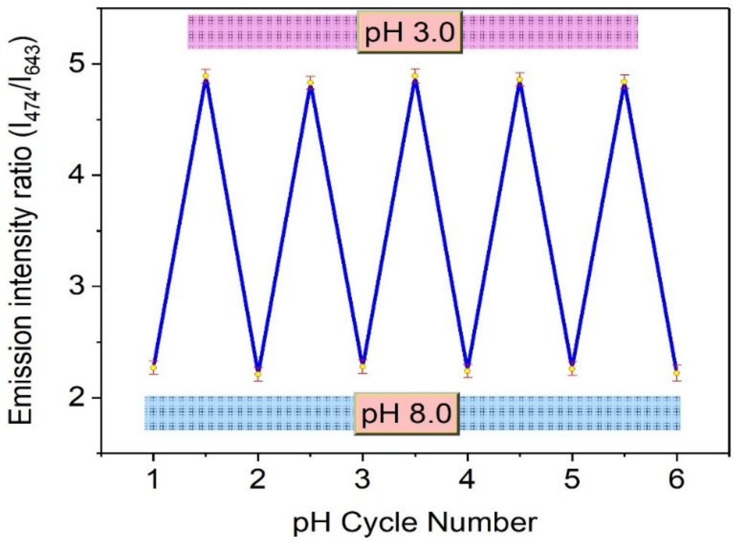

Figure S8. Upconversion emission intensity ratio of 474 nm to 643 nm band, determined in consecutive five pH –cycles within pH 3 to 8.

Table S1. Upconversion luminescence bands, their originating transitions, slope values and theoretical number of pump photons upon 980 nm excitation. The higher slope values indicate that most of the emission bands are originated from efficient successive energy transfer processes.

Group	**Wavelength (nm)**	**Electronic transition**	**Slope-value from Figure 3c**	**Theoretical value**
A	300	$^1I_6 \rightarrow {}^3H_6$	2.54 ± 0.26	≥5
	343	$^1I_6 \rightarrow {}^3F_4$	3.50 ± 0.33	
B	360	$^1D_2 \rightarrow {}^3H_6$	4.76 ± 0.26	≥4
	449	$^1D_2 \rightarrow {}^3H_6$	4.71 ± 0.15	
C	474	$^1G_4 \rightarrow {}^3H_6$	4.72 ± 0.18	≥3
	643	$^1G_4 \rightarrow {}^3F_4$	4.16 ± 0.25	
D	775	$^3H_4 \rightarrow {}^3H_6$	4.0 ± 0.2	≥2
	802	$^3H_4 \rightarrow {}^3H_6$	3.06 ± 0.13	

Table S2. Zeta potentials of PEI-modified nanoparticles in different pH buffers.

pH	**3.0**	**6.0**	**8.0**
Zeta (ζ) potential	+20.91±0.41 mV	+3.37±0.32 mV	-1.49±0.41 mV

References

1. J. B. Pawley, *Handbook of Biological Confocal Microscopy*, 2006.
2. S. Guo, M. K. Tsang, W. S. Lo, J. Hao, and W. T. Wong, *Nanoscale*, 2018, **10**(6), 2790-2803.

3. F. Auzel, *Chem. Rev.*, 2004, **104**, 139–174.